



# CHORUS

This is the accepted manuscript made available via CHORUS. The article has been published as:

## Electron-limiting defect complex in hyperdoped GaAs: The DDX center

Jie Ma and Su-Huai Wei

Phys. Rev. B **87**, 115210 — Published 29 March 2013

DOI: [10.1103/PhysRevB.87.115210](https://doi.org/10.1103/PhysRevB.87.115210)

# Electron-limiting defect complex in hyperdoped GaAs: The DDX center

Jie Ma and Su-Huai Wei

*National Renewable Energy Laboratory, Golden, Colorado 80401, USA*

The physical properties and chemical trends of defects in GaAs under the hyperdoping situation are investigated and found to be very different from those in the impurity limit. We show that at high dopant concentrations, a defect complex denoted as the DDX center becomes the dominant “killer” to limit the electron carrier concentration, whereas in the impurity limit, the electron carrier concentration is usually limited by the well-known DX center. The DDX center shows some opposite chemical trends compared to the DX center. For example, to avoid the DX center, anion site donors are preferred, but to avoid the DDX center, cation site donors are better. Our proposed mechanism is able to explain some puzzling experimental observations.

PACS numbers: 61.72.Bb, 61.72.J-, 61.72.uj, 71.55.Eq

## I. INTRODUCTION

Introducing charged carriers into a semiconductor is a critical process to functionalize the semiconductor for specific electronic or optoelectronic device applications<sup>1,2</sup>. In most cases, this is done through doping. Due to its importance, extensive studies have been carried out to understand the mechanism of doping, including the stability of the defects, the transition energy levels, the microscopic structures of the defects, and the defect charge compensation<sup>3,4</sup>. Most of the previous studies are for defects in the impurity limit and various approaches have been proposed to overcome the doping limit in semiconducting or insulating materials<sup>5</sup>. For many semiconductors, however, hyperdoping (doping to a high concentration) is required to improve the electronic conductivity or modify the host band structure for next-generation electronic and optical devices, such as bipolar transistors, spintronic devices, or high-efficiency solar and photoelectrochemical cells for energy production<sup>6-9</sup>, especially as the size of the devices is reduced to the nanoscale<sup>10,11</sup>.

It is usually assumed that when the dopant concentration increases from the impurity limit to the hyperdoping limit, the general chemical trends of the stability of the defects are preserved, except that defect bands can form through the overlapping of the defect wavefunctions<sup>12,13</sup>. Because of this expectation, understanding obtained through studies of isolated defects in a semiconductor is usually extrapolated to interpret experimental results at high dopant concentrations. However, we will show that this expectation may not be valid, even for some important defects such as DX centers in conventional semiconductor GaAs.

The DX center is an important defect in semiconductors that converts a shallow donor into a deep level<sup>14-17</sup>. Thus it is a major “killer” defect for the saturation of free-electron carrier concentration in the doping process<sup>18-22</sup>. Because of its importance, it has been extensively studied and discussed in GaAs and other III-V and II-VI semiconductors<sup>18-25</sup>. It is well known that the DX center is formed by a large lattice distortion that lowers a conduction-band-derived defect level down into the band gap, which can trap extra electrons. The lowering of the defect level gains electronic energy when it becomes occupied and compensates the energy cost due to the lattice distortion<sup>22</sup>. Several structures for the DX center have been proposed in the literature, such as the broken-bond model (BB-DX) and the  $\alpha$  and  $\beta$  cation-cation bond model (CCB-DX)<sup>18-20,23</sup>. In general, DX centers can be stabilized by pushing up the conduction band either by pressure, alloying, or quantum confinement<sup>16,17,24</sup>. For GaAs and other III-V and II-VI semiconductors, calculations have shown that the cation site donor-induced DX centers are easier to form than the anion site donor-induced ones<sup>23,25,26</sup>.

All the previous studies are for isolated DX centers. This is valid if the doping concentration is in the impurity limit. However, if the dopant concentration is high, the stability and chemical trends observed for the isolated DX center may not hold anymore. This is because when a DX center traps an extra electron and becomes negatively charged, it also creates an ionized defect  $d$ , which donates the electron and is positively charged. In heavily doped GaAs, the Coulomb interaction between the negatively charged DX center and the positively charged donor  $d$  tends to combine them into a new defect complex denoted here as the DDX center, which, as we will show below, becomes the dominant “killer” defect limiting the free-electron carrier concentration and has very different chemical trends compared to the DX center. However, the structural and electronic properties of the DDX center have never been explicitly studied in previous theoretical investigations.

In this paper, using density functional theory (DFT) calculations, we have calculated the formation of the DX and DDX centers in GaAs. We show that the defect chemistry under the hyperdoping situation is indeed different from that in the impurity limit. We calculate both the group-IV donors, such as Si, Ge, and Sn substitution on the Ga site, and the group-VI donors, such as S, Se, and Te substitution on the As site. For the DX center, our calculated results are in agreement with previous calculations. The new DDX center is also a deep-level defect similar to the DX center, but its physical properties and chemical trends are different from those of the DX center. Due to the Coulomb attraction, the formation energy of the DDX center is always lower than that of the DX center. However, because the DX center only involves one dopant atom but the DDX center involves two, the formation of the DDX center is limited by the entropy term. Therefore, the DDX center is negligible in the impurity limit but becomes significant in the hyperdoping case, which limits the free-electron carrier concentration. The anion site dopant-induced DDX centers are easier to form than the cation site dopant-induced ones, which is the opposite of the trend of the DX centers. Therefore, at low dopant concentration, the anion site dopants are better choices to avoid the formation of the DX centers, but at high dopant concentration the cation site dopants are preferred to avoid the DDX centers. Furthermore, to reduce the concentration of the DDX centers in order to get better n-type performance, high-temperature annealing will be helpful. The results can explain some puzzling experimental observations in heavily doped GaAs<sup>27,28</sup>.

## II. METHODS OF CALCULATIONS

The DFT calculations are performed using the local density approximation (LDA)<sup>29</sup> as implemented in the VASP code<sup>30</sup>. The electron-ion interactions are described by projector augmented wave pseudopotentials<sup>31</sup>. The valence

wavefunctions are expanded in a plane-wave basis set with a cutoff energy of 300 eV. We have performed the calculations in a 64-atom supercell with  $4 \times 4 \times 4$   $k$ -point mesh for Brillouin zone integration. We have also tested larger supercells and finer  $k$ -point mesh, and the change of energy difference is not significant. All the atoms in the supercell are allowed to relax until the force on every atom is smaller than 0.02 eV/Å. The calculated lattice constant of GaAs is 5.61 Å, which is in good agreement with the experimental value of 5.65 Å. The calculated band gap is 0.48 eV, while the experimental value is 1.52 eV. Because the formation of DX and DDX centers depends on the band gap, to partially correct the LDA band gap error, an external pressure is applied to increase the calculated band gap to 0.97 eV, closer to the experimental value. We want to point out that the chemical trend studied here is not sensitive to the band gap errors. Without the band gap correction, the formation energies of both DX and DDX centers increase, but all the energy trends discussed in the following section are kept the same.

### III. RESULTS AND DISCUSSIONS

We first discuss the group-IV and group-VI donor-induced DX centers in GaAs. The BB-DX center model is studied here because it is expected to be the more stable one in GaAs<sup>23</sup>. The structures of the group-IV and group-VI donor-induced BB-DX centers are displayed in Fig. 1 (a) and (b), respectively. As discussed before<sup>18,19,23,24</sup>, the bond between the dopant atom and a host atom is broken, and the cation atom is displaced along the [111] direction to the interstitial position. The local symmetry changes from  $T_d$  to  $C_{3v}$  and the defect level converts from shallow to deep, limiting the n-type doping process.

As we discussed above, the  $DX^-$  center is formed by grab an electron from another donor, making it ionized. The reaction is  $2d^0 \rightarrow DX^- + d^+$ , where the positively charged donor and negatively charged DX center do not interact with each other. Following the definition of Chadi and Chang in Ref.[18], the formation energy of the DX center is defined as<sup>32</sup>

$$\Delta E_f(DX) = E(DX^-) + E(d^+) - 2E(d^0), \quad (1)$$

where  $E(DX^-)$ ,  $E(d^+)$ , and  $E(d^0)$  represent the individually calculated total energies of the negatively charged DX center, positively charged and neutral donors in  $T_d$  symmetry, respectively. Negative value will mean the DX center is more stable. Our calculated formation energies for the group-IV and group-VI donor-induced DX centers are presented in Table I. The trends of our calculated results are in good agreement with previous calculations<sup>23</sup>.

Comparing the formation energy of the DX centers induced by the group-IV and group-VI donors, it is clear that the group-IV donor-induced DX centers are more stable than the group-VI donor-induced ones. This is explained by the energy of the lone pair electrons of the DX centers (Fig. 2). For the group-IV dopant case, the lone pair is localized on the displaced dopant atom, while for the group-VI dopant case, it is localized on the displaced Ga atom. The energy of the lone pair DX level depends on the electronegativity of the atom on which the lone pair locates. The larger the electronegativity, the more stable the lone pair is. Therefore, because the group-IV dopant is more electronegative than Ga, the group-IV donor-induced DX centers are in general more stable than those induced by the group-VI donors, which indicates that the anion site donors should be used in lightly doped GaAs.

Next, we check the stability of the DDX structure. With *ab initio* calculations, we have tested various configurations of the DDX centers, and the most stable ones induced by the group-IV and group-VI dopants are displayed in Fig. 1 (c) and (d), respectively. To understand these geometries, we propose a simple model based on the Coulomb interaction and electron counting rule. In GaAs, each bond has two electrons. Since the Ga atom has three valence electrons and As has five, in terms of electron counting, the Ga atom contributes 3/4 electrons and As contributes 5/4 to each bond. When a DX center is formed, a Ga-As bond is broken. According to the electron counting rule, the Ga site needs 5/4 electrons to fill the dangling bond and the As site needs 3/4 electrons. For the group-IV dopant case, the dopant atom replaces the displaced Ga atom. Because the group-IV atom has already one more valence electron than Ga, it only needs  $5/4 - 1 = 1/4$  electrons to fill its dangling bond state; therefore, when an extra electron is captured by the DX center, because the group-IV site traps 1/4 electrons and the As site traps 3/4 electrons to fill their dangling bonds, the group-IV site is  $-1/4$  charged and the As site is  $-3/4$  charged. When the DDX center is formed, the  $+1$  charged donor prefers to stay close to the  $-3/4$  charged As site to maximize the Coulomb attraction, as shown in Fig. 1 (c). For the group-VI dopant, it replaces the As atom. Because it has one more valence electron than As, this site actually donates 1/4 electron to the displaced Ga site when the DX is formed by capturing an extra electron on the displaced Ga site. Therefore, in this case, the group-VI atom site is  $+1/4$  charged, whereas the displaced Ga site is  $-5/4$  charged. When the DDX center is formed, the  $+1$  charged donor prefers to stay close to the  $-5/4$  charged Ga site to maximize the Coulomb attraction, as shown in Fig. 1 (d).

The DDX center is formed from the reaction  $2d^0 \rightarrow DDX$ . In the supercell calculations, initially the two donors are calculated in separate supercells, respectively. After the DDX center is formed, the two dopant atoms are in one

supercell, leaving the other one pure undoped GaAs. Therefore, the formation energy of the DDX center is defined as

$$\Delta E_f(\text{DDX}) = E(\text{DDX}) + E(\text{GaAs}) - 2E(\text{d}^0), \quad (2)$$

where  $E(\text{DDX})$  and  $E(\text{GaAs})$  are the individually calculated total energies of the DDX center and undoped GaAs host, respectively. The results for both group-IV and group-VI dopants are listed in Table I. For all these dopants, the DDX centers are more stable than the DX centers, which indicates attractive Coulomb interaction energy. Specifically, for the group-IV dopant-induced DDX centers, the trend of formation energies stays the same as that of the DX centers. However, for the group-VI dopant case, the DDX center becomes more stable as the dopant size decreases, which is the opposite of the trend of the DX centers. Furthermore, if we compare the formation energies of the DDX centers between the group-IV and group-VI doped systems, we find that the anion site (group-VI) dopant-induced DDX centers are easier to form than the cation site (group-IV) dopant-induced ones, which is again the opposite of the trend of the DX centers.

To further analyze the results, we define the binding energy as

$$\begin{aligned} E_b &= E(\text{DDX}) + E(\text{GaAs}) - E(\text{DX}^-) - E(\text{d}^+) \\ &= \Delta E_f(\text{DDX}) - \Delta E_f(\text{DX}), \end{aligned} \quad (3)$$

The calculated values are also presented in Table I. The more negative value indicates that the binding is stronger. We see that the binding of the group-VI dopant is always stronger than that of the group-IV dopant. For the group-IV dopant, the binding energy is almost the same as the dopant changes. In contrast, the binding of the group-VI dopant becomes stronger as the dopant size decreases. The calculated results are explained as follows: the Coulomb interaction of the DDX center can be given by  $q_1 q_2 / 4\pi\epsilon_0\epsilon r$ , where  $\epsilon_0$  and  $\epsilon$  are the dielectric constants of the vacuum and GaAs, respectively.  $q_1$  and  $q_2$  are the effective charges of the  $\text{DX}^-$  and  $\text{d}^+$ , and  $r$  is the distance between them. The effective charge center of the  $\text{DX}^-$  is on the broken Ga-As bond, closer to As for the group-IV dopant and closer to Ga for the group-VI dopant, whereas the effective  $\text{d}^+$  charge center is on the donor site. For the group-IV dopants, as the distance between the positively charged donor and the negatively charged DX center is relatively large, the Coulomb binding  $\sim -180$  meV is thus relatively weak. Furthermore, because the electronegativities of Si, Ge, and Sn are close and the distance between two dopant atoms is large, the Coulomb binding does not change much when the group-IV dopant changes. For the group-VI dopants, the distance  $r$  is relatively small and the negative charge on the displaced Ga site is large, so its Coulomb binding is strong,  $-250 \sim -660$  meV. As the size of the group-VI atoms decreases from Te to Se to S, the bond length decreases, so the magnitude of the binding energy  $E_b$  increases.

Because the DDX center involves two dopant atoms, it is not easily formed at finite temperature with low dopant concentration because of the entropy contribution. Thus, it is valid in previous studies to neglect the existence of the DDX centers when the dopant concentration is low. However, at high dopant concentration, especially for hyperdoping, the DDX centers will become important defects due to the strong binding energy. To quantify this effect, we consider the effect of the dopant concentration on the population of the DDX center. Assuming no spatial correlation, the concentrations of the regular ( $T_d$  symmetry) donor ( $N_d$ ), the DX center ( $N_{\text{DX}^-}$ ), and the DDX center ( $N_{\text{DDX}}$ ) are given by

$$\begin{aligned} N_d &= N e^{-\Delta H_d / k_B T} \\ N_{\text{DX}^-} &= \alpha N e^{-\Delta H_{\text{DX}^-} / k_B T} \\ N_{\text{DDX}} &= \beta N e^{-\Delta H_{\text{DDX}} / k_B T} \\ N_{\text{tot}} &= N_d + N_{\text{DX}^-} + 2N_{\text{DDX}}, \end{aligned} \quad (4)$$

where  $N$  is the concentration of the host lattice site,  $\alpha$  and  $\beta$  are the site degeneracies for the DX and DDX centers, and  $N_{\text{tot}}$  is the total concentration of the dopant in the system. Note that  $\Delta H_{\text{DDX}} - 2\Delta H_d = \Delta E_f(\text{DDX})$  is just the formation energy of the DDX center defined above. We take the GaAs:Se system as an example. The temperature  $T$  is set to 800 K. The populations of the regular donor, DX center, and DDX center versus the total dopant concentration are plotted in Fig. 3. Because the DX center is less stable for Se doping, there are only a small amount of DX centers for all the dopant concentrations; thus, the DX center can be ignored. The population of the DDX center depends on the dopant concentration. It is clear that at low dopant concentrations, the DDX center hardly exists in the system, thus it can be neglected. However, when the dopant concentration is higher than  $10^{18} \text{ cm}^{-3}$ , the DDX center starts to appear. In hyperdoped systems ( $> 10^{19} \text{ cm}^{-3}$ ), it becomes significant.

The appearance of the DDX centers makes the hyperdoping different from the impurity doping. Because the DDX centers are negligible at low dopant concentration, for shallow donors, the free-electron carrier concentration increases linearly with the dopant concentration. However, in the hyperdoping case, because of the existence of the DDX centers, the free-electron carrier concentration tends to saturate. Furthermore, in the impurity doping case, the anion site

donors should be employed for better n-type performance to avoid the formation of the DX centers. For hyperdoping, however, because the DDX centers are more difficult to form on the cation site, the cation site donors should be better. The appearance of the DDX centers depends on temperature. At higher temperature, the entropy term plays a more important role and therefore the DDX centers start to appear at higher dopant concentration. This indicates that free-electron carrier concentration depends on the annealing temperature. At a fixed dopant concentration, a better n-type material can be achieved by high-temperature annealing.

Our result can explain some puzzling experimental observations. For example, when the dopant (Se or Te) concentration in GaAs is high, it is observed that<sup>27,28</sup> at high annealing temperature the free-carrier concentration increases almost linearly with the dopant concentration, but at low annealing temperature the free-carrier concentration saturates as the dopant concentration is higher than  $10^{19} \text{ cm}^{-3}$ . These observations are in agreement with our results, because at high temperature the DDX center is more difficult to form but at low temperature it can form more easily to limit the free-carrier concentration. Furthermore, the X-ray scattering measurements suggest that at low annealing temperature dopant-pairs along the  $\langle 110 \rangle$ -direction are formed<sup>27</sup>, which is again in agreement with our DDX model of group-VI dopants (see Fig. 1 (d)).

#### IV. SUMMARY

In summary, using first-principles calculations we have calculated the formation of the DX and DDX centers in GaAs. We have shown that the microscopic structure of defects and their chemical trends can be drastically different at low dopant concentration and at high dopant concentration. We find that at high dopant concentration, a new defect complex denoted as the DDX center becomes the dominant free-carrier “killer” defect. The DDX center has opposite site preference to the DX center. The structures for the DDX centers are identified and the general chemical trends are explained in terms of a simple Coulomb interaction model. The mechanism we proposed here is in agreement with previous experimental observations.

#### Acknowledgments

We would like to thank Dr. R Bacewicz, J. Li, W. -J. Yin, and Y. Yan for helpful discussions. The work at NREL was supported by the U.S. Department of Energy under Contract No. DE-AC36-08GO28308.

- 
- <sup>1</sup> S. Sze, *Physics of Semiconductor Devices* (Wiley, New York, 1981), 2nd ed.
- <sup>2</sup> A. S. Grove, *Physics and Technology of Semiconductor Devices* (Wiley, New York, 1967).
- <sup>3</sup> S.-H. Wei, *Comput. Mater. Sci.* **30**, 337 (2004).
- <sup>4</sup> C. G. Van de Walle and J. Neugebauer, *J. Appl. Phys.* **95**, 3851 (2004).
- <sup>5</sup> *Advanced Calculations for Defects in Materials*, edited by A. Alkauskas, P. Deak, J. Neugebauer, A. Pasquarello, and C. G. Van de Walle (Wiley-VCH, New York, 2011).
- <sup>6</sup> Y. Yan, J. Li, S.-H. Wei, and M. M. Al-Jassim, *Phys. Rev. Lett.* **98**, 135506 (2007).
- <sup>7</sup> X. Luo, S. B. Zhang, and S.-H. Wei, *Phys. Rev. Lett.* **90**, 026103 (2003).
- <sup>8</sup> B. K. Newman, M.-J. Sher, E. Mazur, and T. Buonassisi, *Appl. Phys. Lett.* **98**, 251905 (2011).
- <sup>9</sup> M.-J. Sher, M. T. Winkler, and E. Mazur, *MRS Bulletin* **36**, 439 (2011).
- <sup>10</sup> D. Mocatta, G. Cohen, J. Schattner, O. Millo, E. Rabani, and U. Banin, *Science* **332**, 77 (2011).
- <sup>11</sup> A. Sahu, M. S. Kang, A. Kompch, C. Notthoff, A. W. Wills, D. Deng, M. Winterer, C. D. Frisbie, and D. J. Norris, *Nano Lett.* **12**, 2587 (2012).
- <sup>12</sup> E. Ertekin, M. T. Winkler, D. Recht, A. J. Said, M. J. Aziz, T. Buonassisi, and J. C. Grossman, *Phys. Rev. Lett.* **108**, 026401 (2012).
- <sup>13</sup> M. T. Winkler, D. Recht, M.-J. Sher, A. J. Said, E. Mazur, and M. J. Aziz, *Phys. Rev. Lett.* **106**, 178701 (2011).
- <sup>14</sup> D. V. Lang and R. A. Logan, *Phys. Rev. Lett.* **39**, 635 (1977).
- <sup>15</sup> P. M. Mooney, *J. Appl. Phys.* **67**, R1 (1990).
- <sup>16</sup> M. Mizuta, M. Tachikawa, H. Kukimoto, and S. Minomura, *Jpn. J. Appl. Phys.* **24**, L143 (1985).
- <sup>17</sup> M. F. Li, P. Y. Yu, E. R. Weber, and W. Hansen, *Appl. Phys. Lett.* **51**, 349 (1987).
- <sup>18</sup> D. J. Chadi and K. J. Chang, *Phys. Rev. Lett.* **61**, 873 (1988).
- <sup>19</sup> D. J. Chadi and K. J. Chang, *Phys. Rev. B* **39**, 10063 (1989).
- <sup>20</sup> C. H. Park and D. J. Chadi, *Phys. Rev. B* **54**, R14246 (1996).
- <sup>21</sup> S. B. Zhang, S.-H. Wei, and A. Zunger, *Phys. Rev. Lett.* **84**, 1232 (2000).
- <sup>22</sup> S.-H. Wei and S. B. Zhang, *Phys. Rev. B* **66**, 155211 (2002).
- <sup>23</sup> M.-H. Du and S. B. Zhang, *Phys. Rev. B* **72**, 075210 (2005).
- <sup>24</sup> J. Li, S.-H. Wei, and L.-W. Wang, *Phys. Rev. Lett.* **94**, 185501 (2005).
- <sup>25</sup> M.-H. Du, *Appl. Phys. Lett.* **92**, 181908 (2008).
- <sup>26</sup> L. V. Besteiro, L. Tortajada, M. L. Tiago, L. J. Gallego, J. R. Chelikowsky, and M. M. G. Alemany, *Phys. Rev. B* **81**, 121307 (2010).
- <sup>27</sup> T. Slupinski and E. Zielinska-Rohozinska, *Thin Solid Films* **367**, 227 (2000).
- <sup>28</sup> C. S. Fuller and K. B. Wolfstirn, *J. Appl. Phys.* **34**, 2287 (1963).
- <sup>29</sup> W. Kohn and L. J. Sham, *Phys. Rev.* **140**, A1133 (1965).
- <sup>30</sup> G. Kresse and J. Furthmuller, *Phys. Rev. B* **54**, 11169 (1996).
- <sup>31</sup> G. Kresse and D. Joubert, *Phys. Rev. B* **59**, 1758 (1999).
- <sup>32</sup> For shallow defect with  $U = 0$ , *i.e.*,  $E(d^+) + E(d^-) = 2E(d^0)$ , this definition is equivalent to  $\Delta E_f(DX) = E(DX^-) - E(d^-)$ , which is used in Ref[23–25].

TABLE I: The formation energies of the DX and DDX centers induced by the group-IV and group-VI dopants. Negative value indicates the DX or DDX centers are stable. The DDX binding energies are also presented.

Dopant	$\Delta E_f(\text{DX})$ (meV)	$\Delta E_f(\text{DDX})$ (meV)	$E_b$ (meV)
Si	158	-24 <sup>a</sup>	-182
Ge	-69	-257	-188
Sn	12	-173	-185
S	369	-296	-665
Se	235	-229	-464
Te	46	-200	-246

<sup>a</sup>The Si-induced CCB-DDX is 110 meV more stable than the BB-DDX presented here. It does not change the fact that the DDX center is more easily formed on the anion site.

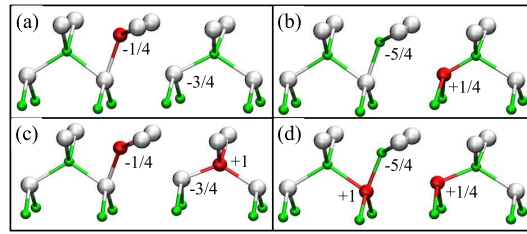


FIG. 1: The structures of the DX and DDX centers in GaAs. (a) The structure of the group-IV dopant-induced DX center; (b) the structure of the group-VI dopant-induced DX center; (c) the structure of the group-IV dopant-induced DDX center; (d) the structure of the group-VI dopant-induced DDX center. The numbers indicate the net charge of the atoms with dangling bonds and the ionized donor, according to the electron counting rule. The white, green, and red balls represent As, Ga, and dopant atoms, respectively.

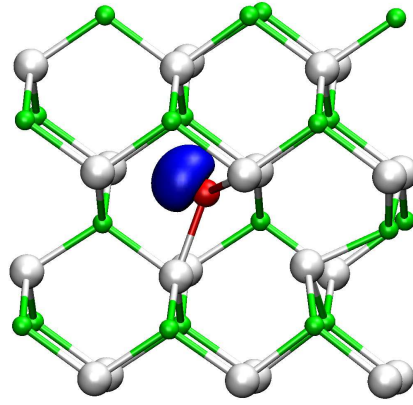


FIG. 2: The charge density of the defect state of the group-IV dopant-induced DX center. The charge density of the group-VI dopant-induced DX center is similar. The white, green, and red balls represent As, Ga, and dopant atoms, respectively.

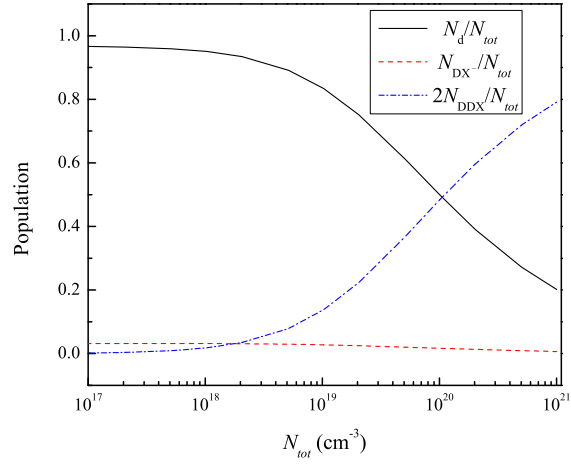


FIG. 3: The populations of the regular donor, DX center and DDX center as a function of the total dopant concentration. At low dopant concentration, due to the entropy term, the DDX center is negligible. However, for hyperdoping, the DDX center becomes dominant.